Scandium on the formation of in situ TiB_2 particulates in an aluminum matrix

Dan Huang
School of Engineering Technology, Purdue University, West Lafayette, Indiana 47906, USA

David Yan
Department of Aviation and Technology, San Jose State University, San Jose, California 95192, USA

Siming Ma and Xiaoming Wang[a)]
School of Engineering Technology, Purdue University, West Lafayette, Indiana 47906, USA

(Received 9 May 2018; accepted 5 June 2018)

TiB_2 particulates were formed in situ in an aluminum matrix via chemical reactions between an aluminum melt and the mixture of K_2TiF_6 and KBF_4 salts. Different effects of Sc addition on the formation of the TiB_2 particulates were revealed depending on the participation of Sc at different stages of the formation of the particulates. The metal–salt reactions resulted in boride layers along the α-Al grain boundaries in the presence of Sc, while the addition of Sc after the metal–salt reactions broke up the boride layers improving the dispersion of the TiB_2 particulates to a limited degree. Sc promoted the growth of the TiB_2 particulates, resulting in the coarsening of TiB_2 particulates. The participation of Sc in the formation of TiB_2 particulates altered the coarsening of the TiB_2 particulates, resulting in different morphologies of the TiB_2 particulates depending on the participation of Sc in the formation of the TiB_2 particulates at different stages.

I. INTRODUCTION

Aluminum alloys reinforced with ceramic particulates, aluminum metal matrix composites (MMCs),[1,2] show a high potential in meeting the ever-increasing demand for property improvement, such as high strength and high modulus, from the fast growing aerospace, electronics, and automotive industries.[1–4] Aluminum alloys, as matrices, are featured with low density, high thermal conductivity, and plasticity. Meanwhile, the ceramic particulates offer high strength and moduli. Among various ceramic reinforcements, TiB_2 particulates have attracted a great deal of attention due to their high strength, hardness, and strong covalent bonding with the aluminum matrix.[5–15] The most attractive property of TiB_2 as reinforcement is its good wettability by an aluminum melt, resulting in strong bonding to the aluminum matrix, which transfers stress from the matrix to the reinforcing particulates effectively in service with improved strength. A good wettability is also a key factor for obtaining uniform dispersion of the reinforcing particulates and therefore homogeneous properties of the composites. In comparison, other ceramic particulates, such as Al_2O_3, SiC, etc., are not wetted by an aluminum melt, causing difficulties in dispersion into an aluminum melt and therefore weak matrix/reinforcement interfacial bonding and possible premature failure.[1,2,16–19]

TiB_2 particulates can be introduced into an aluminum matrix as preformed particulates (ex situ) or formed in situ in the matrix. In situ fabrication eliminates possible oxygen contamination, producing a clean TiB_2/Al interface and, therefore, strong TiB_2/Al interfacial bonding after solidification.[5–14] A popular method in synthesizing in situ TiB_2 particulates is through salt–metal reactions by adding mixed K_2TiF_6 and KBF_4 salts into an aluminum alloy melt derived from the production of Al–Ti–B type master alloys for grain refinement.[20] From the beneficial effects of TiB_2 in aluminum grain refinement, the advantages of TiB_2 particulates as reinforcement are obvious.[5,6] Possible chemical reactions between an aluminum melt and mixed salts are presented as reactions (1)–(3) without the consideration of AlB_2 formation, where Ti and B are reduced from fluoride salts by aluminum.[10] The Ti and B in solution will then form TiB_2 particulates in an Al melt. The formation of AlB_2 as a separate phase or in solid solution with TiB_2 is possible by considering the production of Al–B master alloys from reactions of KBF_4 and an aluminum melt.[21–24]

$$K_2TiF_6 + 2KBF_4 + 10/3Al = TiB_2 + 4/3(3KF \cdot AlF_3) + 2AlF_3 \quad , \tag{1}$$

[a)]Address all correspondence to this author.
e-mail: wang1747@purdue.edu
DOI: 10.1557/jmr.2018.208

$$2K_2TiF_6 + 2KBF_4 + 23/3Al = TiB_2 + Al_3Ti + 2(3KF \cdot AlF_3) + 8/3AlF_3 \quad , \tag{2}$$

$$K_2TiF_6 + 13/3Al = Al_3Ti + 2/3(3KF \cdot AlF_3) + 2/3AlF_3 \quad . \tag{3}$$

According to reactions (1)–(3), TiB_2 and Al_3Ti particulates in a variable ratio can be produced by reactions between an aluminum melt and a mixture of K_2TiF_6 and KBF_4 salts. The formation of Al_3Ti particulates can be avoided by varying the K_2TiF_6/KBF_4 ratio to reaction (1). However, a small amount of excess Ti in solution is beneficial for the dispersion of TiB_2 particulates by promoting the nucleation of aluminum grains on the TiB_2 particulates.[7,25] Among the reaction products, TiB_2 is the most stable phase thermodynamically because of its lowest standard free energy change of formation.[26] However, it is unavoidable to form AlB_2 intrinsic to the chemical reactions, where aluminum participates in the reactions with boron.[12,13] Different diborides form solid solutions in the aluminum melt with a high tendency to transform into mixtures of diborides, TiB_2, AlB_2, etc, which is not widely agreed.[5,12,13] TiB_2 is generally treated as the final product in the aluminum melt due to difficulties in distinguishing different diboride phases in an aluminum alloy. The beneficial effects of adding TiB_2 particulates into aluminum alloys have been reported despite the debate about phase formation.[18,19,27] However, the complicated chemical reactions between the salts and aluminum melts and the exothermal nature of the reactions lead to difficulties in controlling the size and morphology of the TiB_2 particulates, which must be resolved before a wide spread application of in situ TiB_2 particulate reinforced aluminum MMCs.

Efforts on producing uniform dispersion of fine in situ TiB_2 particulates have been made mainly through altering the reaction chemistry and applying mechanical agitation. The latter includes mechanical shearing, ultrasonic sonication, electromagnetic stirring, etc., leading to an improved dispersion of the TiB_2 particulates and therefore increased mechanical properties.[26,28,29] Meanwhile, the former focuses on the effects of alloying elements on the growth and dispersion of the in situ TiB_2 particulates.[10,30–36] The effects of different alloying elements have been revealed as either forming solid solutions with TiB_2 leading to coarsening or modifying the interfacial energies to promote the nucleation of the TiB_2 particulates, resulting in fine sized particulates. Specifically, magnesium as an alloying element promotes the nucleation of TiB_2 particulates, while zirconium leads to coarse TiB_2 particulates. Interestingly, TiB_2 particulates also modify the morphology of eutectic Si in an Al–Si alloy.[36] The addition of alloying elements in modifying the in situ TiB_2 particulates also resulted in the increase of mechanical properties.[30–36]

By considering the significant strengthening effects of Sc in aluminum alloys and the increasing applications of Al alloys containing Sc,[36–38] understanding the effects of Sc on the formation of in situ TiB_2 particulates becomes imminent. However, there is hardly information available about the effects of Sc on the formation of TiB_2 particulates. Sc forms Al_3Sc in aluminum either as a strong aluminum grain refiner or dispersoid for precipitation hardening depending on its concentration in an alloy.[37] As reported, when being added into the A356 alloy, Sc has combined effects of being an effective grain refiner as well as Si modifier, modifying the morphology of eutectic Si from needle-like to spheroidal particulates.[38]

From the above review, the addition of TiB_2 particulates into aluminum alloys is effective in strengthening the alloys. Additionally, there is a possibility of adding Sc to increase the properties of the in situ TiB_2 particulate reinforced aluminum MMCs. However, information on the effects of Sc addition on the formation and dispersion of the TiB_2 particulates in Al–TiB_2 composites is lacking, which is the knowledge gap that this article tries to fill.

II. EXPERIMENTAL PROCEDURES

A series of in situ TiB_2 particulate reinforced aluminum MMCs were fabricated with the modification of Sc addition. Pure aluminum (99.99% purity) was placed in a graphite crucible and melted inside an electrical resistant furnace. K_2TiF_6 and KBF_4 salts were used to introduce alloying elements Ti and B. Sc was deployed as an Al–2 wt% Sc master alloy. Al–TiB_2–Sc alloys with 5 wt% TiB_2 particulates and 0.2 wt% Sc were designed. As listed in Table I, an Al–2 wt% Sc master alloy was added under three different sequences to evaluate the effects of Sc addition at different stages of the reactions between the salts and the aluminum melt. When adding

TABLE I. Experimental details for producing Al–TiB_2 (Al–TiB_2–Sc) MMCs.

Composites	Sample no.	Percentage of Sc added as Al–2 wt% Sc		Holding time (min)
		Before reaction	After reaction	
Al–TiB_2	1	...	...	15
	2	...	...	60
	3	0.2	...	15
	4	0.2	...	60
Al–TiB_2–Sc	5	...	0.2	15
	6	...	0.2	60
	7	0.1	0.1	15
	8	0.1	0.1	60

the salts and the Al–Sc master alloy, manual stirring was applied to alleviate the possible agglomeration of reaction products. The reaction temperature was set to 820 °C when the raw materials were melted and alloying elements were added. A holding time for the chemical reaction were set as 15 and 60 min to study their effects on the reaction products. This is based on microstructure analysis showing a 60 min holding time leading to a better dispersion of TiB_2 particulates, whereas a holding time longer than 60 min might not be suitable, as reported by Birol.[21,22] Salt products on top of the melt were decanted before casting the melt into a steel mold. A pouring temperature was chosen as 720 °C and the melt was poured into a steel mold and cooled down to the room temperature. The process is shown in Fig. 1 schematically.

After casting, the ingots were sectioned, ground, polished, and etched following a standard procedure for metallurgical sample preparation for scanning electron microscopy (SEM) and energy dispersive X-ray (EDX) analysis. The SEM images were taken by using an FEI 3D Quanta Dual Beam SEM (ThermoFisher Scientific, Hillsboro, Oregon) operated at 20 kV. Secondary electron images (SEIs) were also taken on deep-etched samples that were prepared by submerging the samples into a solution that consists of 250 mL methanol, 10 g iodine, and 25 g tartaric for 50–60 min, and soaking the samples in acetone until the solvent was clear. The etched samples were then rinsed with acetone and dried up for SEM examination. EDX analysis was performed to reveal the compositions of the particulates.

III. RESULTS AND DISCUSSION

The overall dispersion of the in situ TiB_2 particulates in the aluminum matrix is presented in Figs. 2(a)–2(h),

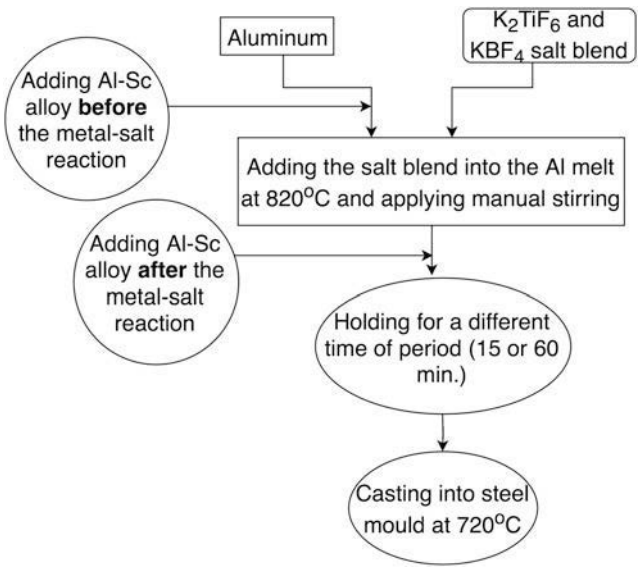

FIG. 1. Schematic processing chart showing the participation of Sc in different stages of the salt–metal reaction.

the back-scattered electron images (BEIs) of eight samples in Table I under a SEM. These images are featured with clusters of diboride particulates along the aluminum grain boundaries, in accordance with the typical dispersion of the diboride particulates in aluminum master alloys, evidencing the weak ability of TiB_2 particulates in nucleating aluminum grains in solidification.[10,11,25,39] The TiB_2 particulates were therefore pushed by the solidifying front of the α-Al grains to the aluminum grain boundaries during solidification.[7,8,10–12,40,41] The only noticeable difference in the images caused by Sc is the different thickness of the TiB_2 layers.

Figures 2(a) and 2(b) are the micrographs of the in situ Al–TiB_2 composites produced without the addition of Sc for a holding time of 15 and 60 min (i.e., Samples 1 and 2), respectively. TiB_2 particulates agglomerate along the α-Al grain boundaries under these conditions. Figures 2(c) and 2(d) show the micrographs of Samples 3 and 4, in which Sc was participating in the metal–salt reactions for a holding time of 15 and 60 min. It can be found from Fig. 2(c) that the TiB_2 particulates tend to agglomerate into layers at the α-Al grain boundaries. This indicates that the participation of Sc in the metal–salt reactions results in a different way of agglomeration of the TiB_2 particulates along the α-Al grain boundaries from the one without Sc addition in Fig. 2(a). Figures 2(e) and 2(f) show the BEIs of Samples 5 and 6, which have Sc added after the metal–salt reactions for a holding time of 15 and 60 min, respectively. By comparing Figs. 2(b)–2(f) (Samples 2 and 6) with the same holding time but under different Sc addition sequences, it is clear that TiB_2 particulates are dispersed rather broadly in Fig. 2(f) than in Fig. 2(b), though the particulates still agglomerated along the α-Al grain boundaries. These results suggest that the addition of Sc after the metal–salt reactions promotes the dispersion of TiB_2 particulates though still along the α-Al grain boundaries comparing with the dispersion of TiB_2 particulates when Sc was participating in the metal–salt reactions. Figures 2(g) and 2(h) present the BSIs of Samples 7 and 8, with the addition of Sc both before and after the metal-salt reactions for holding times of 15 and 60 min, respectively. It is evident that the agglomeration of the TiB_2 particulates alleviated in Fig. 2(h) (Sample 8) compared to Fig. 2(b) (Sample 2).

In brief, the addition of Sc influences the dispersion of the in situ TiB_2 particulates to a certain degree. To be specific, the participation of Sc in the metal–salt reactions causes a layer-like agglomeration of the TiB_2 particulates along the α-Al grain boundaries, while the addition of Sc after the reactions (without the participation of Sc in the metal–salt reactions) alleviates the agglomeration at the grain boundaries.

Figures 3(a)–3(h) are the SEIs of deep-etched Samples 1–8, showing the overall morphologies of the in situ TiB_2 particulates at the Al grain boundaries. Hexagonal TiB_2

particulates in the Al–TiB_2 composites are revealed in all the samples, in agreement with other findings.[26,42–44] The growth of the in situ TiB_2 particulates in the absence of Sc with respect to holding time is not clear by comparing Figs. 3(a) and 3(b). In Fig. 3(a), most of the individual TiB_2 particulates are blocky in submicrometer sizes and only a small portion of the TiB_2 particulates have grown into sizes near 2 μm, similar to the TiB_2 particulates in Fig. 3(b). The result indicates that the effects of the holding time on the growth of the TiB_2 particulates are limited in the absence of Sc. In comparison, Sc addition resulted in the growth of the in situ TiB_2 particulates in different ways depending on the sequence of the addition of Sc and, therefore, its participation in the formation of the TiB_2 particulates at different stages, which is to be discussed in the following paragraphs.

The participation of Sc in the metal–salt reactions resulted in the growth of the TiB_2 particulates for both

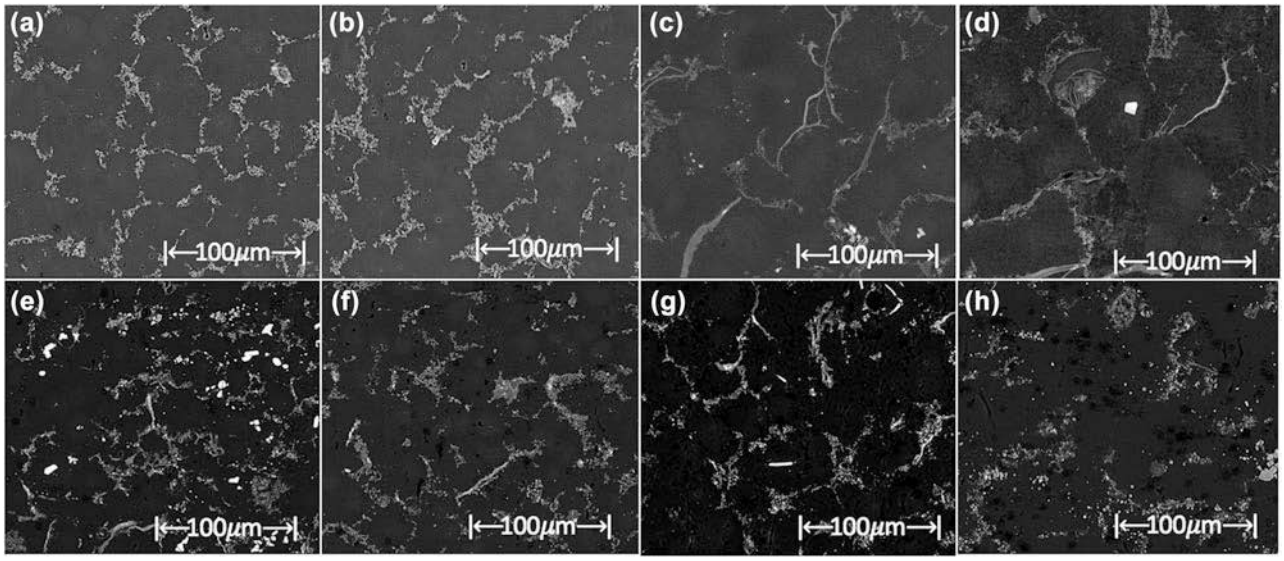

FIG. 2. BSE images of Samples 1–8 showing the dispersion of in situ diboride particles: (a) No addition of Sc (15 min); (b) No addition of Sc (60 min); (c) Adding Sc before the metal–salt reaction (15 min); (d) Adding Sc before the metal–salt reaction (60 min); (e) Adding Sc after the metal–salt reaction (15 min); (f) Adding Sc after the metal–salt reaction (60 min); (g) Adding Sc both before and after the metal–salt reaction (15 min); (h) Adding Sc both before and after the metal–salt reaction (60 min).

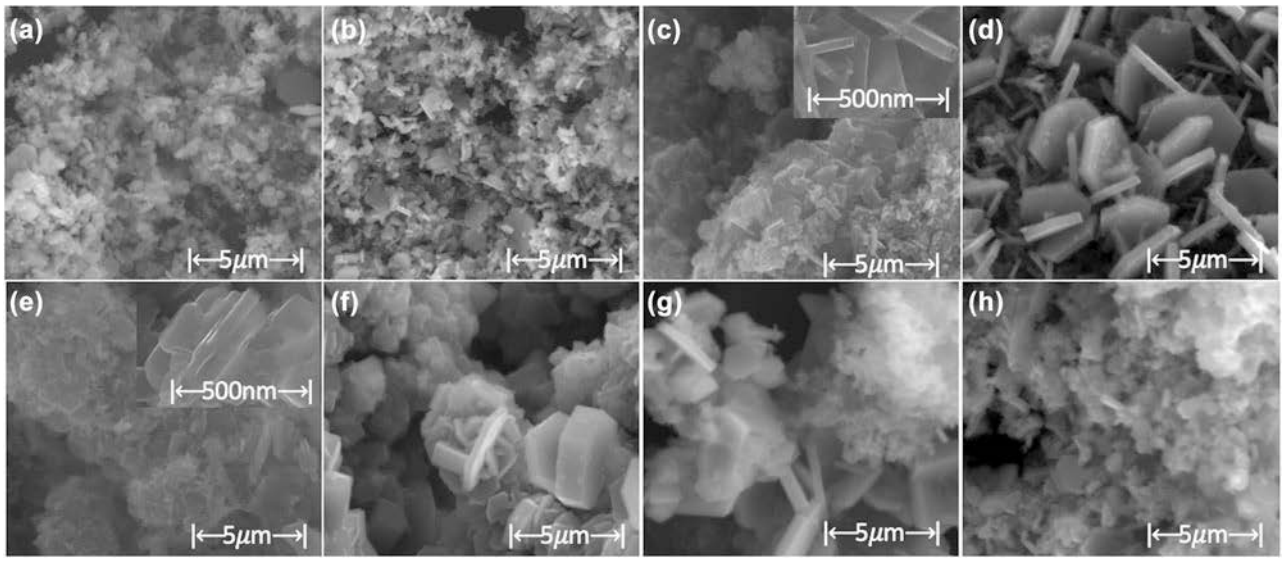

FIG. 3. SEIs of deep-etched Samples 1–8 showing the morphologies of in situ diboride particles: (a) No addition of Sc (15 min); (b) No addition of Sc (60 min); (c) Adding Sc before the metal–salt reaction (15 min); (d) Adding Sc before the metal–salt reaction (60 min); (e) Adding Sc after the metal–salt reaction (15 min); (f) Adding Sc after the metal–salt reaction (60 min); (g) Adding Sc both before and after the metal–salt reaction (15 min); (h) Adding Sc both before and after the metal–salt reaction (60 min) (Inserted figures in (c) and (e) are magnified typical TiB_2 particles).

holding times of 15 and 60 min, which is clear by comparing Figs. 3(c) and 3(d) to 3(a) and 3(b), respectively. Sc promotes the growth of TiB_2 plates through fusion at a short holding time (15 min) and individual plates at a longer holding time (60 min). The effects of holding time on the morphologies of the in situ TiB_2 particulates are clear by comparing Figs. 3(c) and 3(d). A longer holding time of 60 min resulted in the growth of the TiB_2 particulates into about 5 μm in size in Fig. 3(d) from about 2 μm in Fig. 3(c). No obvious growth of the thickness of the hexagonal TiB_2 disks was observed with the increase of holding time, resulting in disks with a larger aspect ratio. These results suggest that the participation of Sc in the metal–salt reactions promotes preferentially the growth of the {0001} planes of the TiB_2 particulates in such a way that it restricts the growth in the [0001] direction comparatively.[5]

When Sc was added after the metal–salt reactions, TiB_2 particulates tend to grow together by {0001} planes at a short holding time (15 min), which is clear in the inset in Fig. 3(e). It can be attributed to that Sc modifies the {0001} planes of the TiB_2 particulates.[5] The growth of the TiB_2 particulates has reached a completion after 60 min, evidenced by the perfect hexagonal shape of the particulates in Fig. 3(f). The growth of TiB_2 particulates is affected largely by the addition sequence of Sc, i.e., the participation in metal–salt reactions or modification of the particulate surfaces. From Fig. 3(e) (Sample 5), it can be found that a large amount of TiB_2 particulates tend to grow up with a blocky morphology with a 15 min holding time. When the holding time increased to 60 min, the TiB_2 particulates coarsened to size of several micrometers and remained blocky. Therefore, it can be proposed that when adding Sc after the metal–salt reactions (without Sc participating in metal–salt reactions), Sc promotes the coarsening of the TiB_2 particulates in all crystal directions though growth or coalescence.

The effects of adding Sc half amount before and the rest half after the metal–salt reactions resulted in TiB_2 particulates in different sizes, which may grow after a longer holding time, as shown in Figs. 3(g) and 3(h). Figure 3(g) shows only a portion of the TiB_2 particulates have grown up to disks about 5 μm, meanwhile the rest are in smaller sizes agglomerated together. A longer holding time (60 min) promoted the growth of the smaller particulates as shown in Fig. 3(h).

Figure 4 is a high magnification SEI of Sample 5 produced by adding Sc after the metal–salt reactions, and Figs. 5(a) and 5(b) are the illustrations of the coarsening of the in situ TiB_2 particulates. As indicated by arrows in Fig. 4, TiB_2 particulates grew in a layer-by-layer manner along the axis of the hexagonal disks. The particulates may grow into a rod-like shape, which is indicated by arrow 1 in Fig. 4 and in Fig. 5(a) or

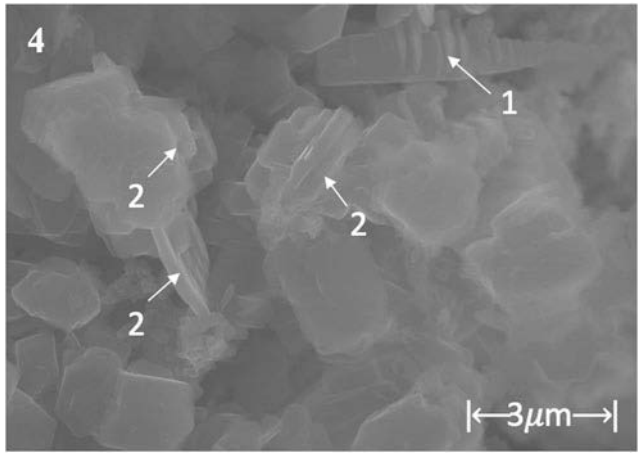

FIG. 4. High magnification SEI of deep-etched Sample 5 showing coarse TiB_2 particles: Arrow (1) rod-like TiB_2 particles; Arrow (2) terrace-like blocky TiB_2 particles.

a terrace-like blocky shape, which is shown by arrow 2 in Fig. 4 and in Fig. 5(b). In Fig. 5(a) (also see arrow 1 in Fig. 4), TiB_2 particulates were growing together separately along a rod-like base parallel to each other. On the other hand, in Fig. 5(b) (also see arrow 2 in Fig. 4), TiB_2 particulates were coalescing upon each other without a distance between neighboring TiB_2 disks [arrow 1 in Figs. 4 and 5(a)]. However, these two growing behaviors of TiB_2 particulates still need further investigation.

By comparing Fig. 4 (Sample 5) and Fig. 3(c) (Sample 3), the coarsening mechanism is not applicable to Sample 3 that was produced by adding Sc before the metal–salt reactions, i.e., the participation of Sc in the metal–salt reactions does not result in similar coarsening of the TiB_2 particulates. The coarsening of the TiB_2 particulates is a direct effect of the modification of the surfaces of the TiB_2 particulates by Sc after the formation of TiB_2 particulates. By considering the high stability of TiB_2 in an aluminum melt,[25] the Ostwald ripening process is unlikely to happen, which is supported by the current results. Therefore, it can be elucidated that Sc modifies the surface of the TiB_2 particulates promoting coarsening of the particulates through a stacking process, i.e., coarsening by stacking TiB_2 disks on their hexagonal surfaces.

Figure 6(a) shows a magnified SEI of deep-etched Sample 4 with an EDX spectrum of a typical TiB_2 cluster from point 1 in the image of Fig. 6(b). EDX spectra from other four locations gave similar compositions to Fig. 6(b). Sc was detected in all the five coarse particulates. EDX analysis validates the participation of Sc in the coarsening of the in situ TiB_2 particulates by modifying the reaction chemistry and the surface energy of the TiB_2 particulates. However, a detailed mechanism about the influence of the Sc during the reaction is still not clear and that requires further investigation.

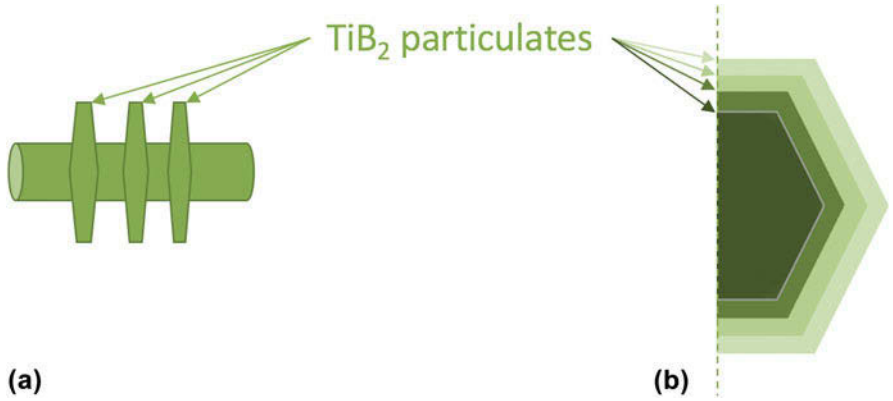

FIG. 5. Schematic drawings of the coarsening mechanisms: (a) rod-like shape and (b) terrace-like block shape.

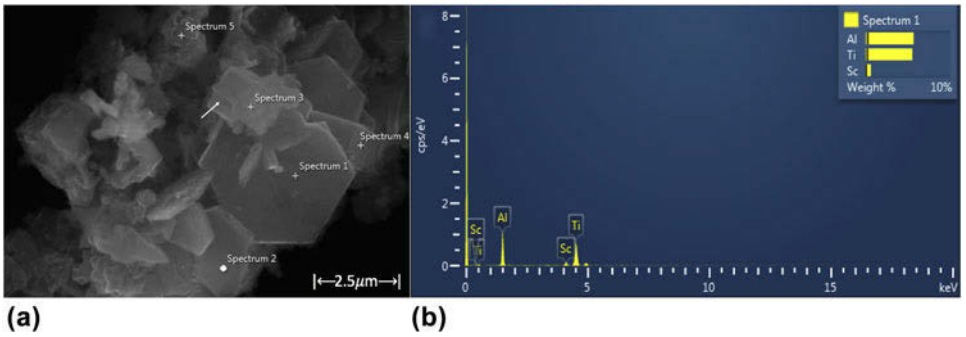

FIG. 6. Magnified SEI of deep-etched Sample 4 (a) with an EDS spectrum (b).

IV. CONCLUSIONS

In situ TiB_2 particulates were produced successfully in an aluminum matrix by the reactions of aluminum and a mixture of K_2TiF_6 and KBF_4 salts with the addition of Sc at different stages of the metal–salt reactions. TiB_2 particulates agglomerated along the Al grain boundaries in all Al–TiB_2–Sc MMCs and the distribution and growth of the TiB_2 particulates were influenced by the presence of Sc during or after the metal–salt reactions. The addition of Sc resulted in the coarsening of TiB_2 particulates, regardless of the participation of the Sc in the metal–salt reactions or not. The participation of Sc in the metal–salt reactions resulted in the formation of petal-like particulates, meanwhile, the addition of Sc after the metal–salt reactions led to the formation of coarse TiB_2 terraces bonded by the large surfaces of the individual TiB_2 disks. Sc also plays a role in promoting the growth of the {0001} planes when participated in the metal–salt reactions. By contrast, the TiB_2 particulates are blocky terraces, when the addition of Sc was made after the metal–salt reactions. EDX analysis validated the existence of Sc in coarse TiB_2 particulates and evidence of an active role of Sc in the formation of the in situ TiB_2 particulates. The paper focuses on the effects of Sc on the formation of in situ TiB_2 particulates without considering possible effects on the mechanical properties of the MMCs.

ACKNOWLEDGMENT

The authors would like to acknowledge AMG Aluminum North America for providing salts for the research.

REFERENCES

1. S.C. Tjiong and Z.Y. Ma: Microstructural and mechanical characteristics of in situ metal matric composites. *Mater. Sci. Eng., R* **29**, 49 (2000).
2. D.J. Lloyd: Particulate reinforced aluminium and magnesium matrix composites. *Int. Mater. Rev.* **39**, 1 (1994).
3. S.V. Prasad and R. Asthana: Aluminum metal-matrix composites for automotive application: Tribological considerations. *Tribol. Lett.* **17**, 445 (2004).
4. I.A. Ibrahim and F.A. Mohamed: Particulate reinforced metal matrix composites—A review. *J. Mater. Sci.* **26**, 1137 (1991).
5. L. Arnberg, L. Bäckerud, and H. Klang: Intermetallic particulates in Al–Ti–B-type master alloys for grain refinement of aluminium. *Met. Technol.* **9**, 7 (1982).
6. G.P. Jones and J. Pearson: Factors affecting the grain-refinement of aluminum using titanium and boron additives. *Metall. Trans. B* **7**, 223 (1976).
7. X. Wang, J. Song, W. Vian, H. Ma, and Q. Han: The interface of TiB_2 and Al_3Ti in molten aluminum. *Metall. Mater. Trans. B* **47**, 3285 (2016).

8. M.M. Guzowski, G.K. Sigworth, and D.A. Sentner: The role of boron in the grain. *Metall. Trans. A* **18**, 603 (1987).
9. D.G. McCartney: Grain refining of aluminium and its alloys using inoculants. *Int. Mater. Rev.* **34**, 247 (1989).
10. X. Wang, R. Brydson, A. Jha, and J. Ellis: Microstructural analysis of Al alloys dispersed with TiB_2 particulate for MMC application. *J. Microsc.* **196**, 137 (1999).
11. C.S. Ramesh, S. Pramod, and R. Keshavamurthy: A study on microstructure and mechanical properties of Al6061-TiB2 in situ composites. *Mater. Sci. Eng., A* **528**, 4152 (2011).
12. X. Wang and Q. Han: Relationship of diboride phases in Al–Ti (Zr)–B alloys. *Mater. Sci. Technol.* **31**, 874 (2015).
13. J. Fjellstedt and A. Jarfors: On the precipitation of TiB_2 in aluminum melts from the reaction with KBF_4 and K_2TiF_6. *Mater. Sci. Eng., A* **413–414**, 527 (2005).
14. S. Suresh, N. Shenbaga, and V. Moorthi: Aluminium–titanium diboride (Al–TiB_2) metal matrix composites: Challenges and opportunities. *Procedia Eng.* **38**, 89 (2012).
15. Q. Zhang, G. Wu, G. Chen, L. Jiang, and B. Luan: The thermal expansion and mechanical properties of high reinforcement content SiCp/Al composites fabricated by squeeze casting technology. *Composites, Part A* **34**, 1023 (2003).
16. Z. Liu, M. Rakita, W. Xu, X. Wang, and Q. Han: Ultrasound assisted salts-metal reaction for synthesizing TiB_2 particulates at low temperature. *Chem. Eng. J.* **263**, 317 (2015).
17. A. Mortensen and I. Jin: Solidification processing of metal matrix composites. *Int. Mater. Rev.* **37**, 101 (1992).
18. P. Davies, J.L.F. Kellie, and J.V. Wood: Development of cast aluminum metal matrix composites. *Key Eng. Mater.* **77–78**, 357 (1992).
19. A. Kennedy, A. Karantzalis, and S. Wyatt: The microstructure and mechanical properties of TiC and TiB_2-reinforced cast metal matrix composites. *J. Mater. Sci.* **4**, 933 (1999).
20. J.V. Wood, P. Davies, and J.L.F. Kellie: Properties of reactively cast aluminium–TiB_2 alloys. *Mater. Sci. Technol.* **9**, 833 (1993).
21. Y. Birol: An improved practice to manufacture Al–Ti–B master alloys by reacting halide salts with molten aluminium. *J. Alloys Compd.* **420**, 71 (2006).
22. Y. Birol: Improved halide salt process to produce Al–B master alloys. *Mater. Sci. Technol.* **12**, 1846 (2011).
23. X. Wang: The formation of AlB_2 in an Al–B master alloy. *J. Alloys Compd.* **403**, 283 (2005).
24. X. Wang: Boride phase formation in the production of Al–B master alloys. *J. Alloys Compd.* **722**, 302 (2017).
25. X. Wang, Z. Liu, W. Dai, and Q. Han: On the understanding of aluminum grain refinement by Al–Ti–B type master alloys. *Metall. Mater. Trans. B* **46**, 1620 (2015).
26. P. Moldovan, M. Butu, G. Popescu, M. Buzatu, E. Usurelu, V. Soare, and D. Mitrica: Thermodynamics of interactions in Al–K_2TiF_6–KBF_4 system. *Rev. Chim. (Bucharest, Rom.)* **9**, 828 (2010).
27. S.C. Tjong, G.S. Wang, and Y.W. Mai: High cycle fatigue response of in situ Al-based composites containing TiB_2 and Al_2O_3 submicron particulates. *Compos. Sci. Technol.* **65**, 1537 (2005).
28. S. Agrawal, A. Ghose, and I. Chakrabarty: Effect of rotary electromagnetic stirring during solidification of in situ Al–TiB_2 composites. *Mater. Des.* **113**, 195 (2017).
29. F. Chen, Z. Chen, F. Mao, T. Wang, and Z. Cao: TiB_2 reinforced aluminum based in situ composites fabricated by stir casting. *Mater. Sci. Eng., A* **625**, 357 (2015).
30. M.A. Herbert, R. Maiti, R. Mitra, and M. Chakraborty: Wear behaviour of cast and mushy state rolled Al–4.5Cu alloy and in situ Al4.5Cu–5TiB_2 composite. *Wear* **265**, 1606 (2008).
31. S. Kumar, M. Chakraborty, V. Subramanya Sarma, and B.S. Murty: Tensile and wear behaviour of in situ Al–7Si/TiB_2 particulate composites. *Wear* **265**, 134 (2008).
32. A. Mandal, R. Maiti, M. Chakraborty, and B.S. Murty: Effect of TiB_2 particulates on aging response of Al–4Cu alloy. *Mater. Sci. Eng., A* **386**, 296 (2004).
33. R. Taghiabadi, M. Mahmoudi, M. Emamy Ghomy, and J. Campbell: Effect of casting techniques on tensile properties of cast aluminium alloy (Al–Si–Mg) and TiB_2 containing metal matrix composite. *Mater. Sci. Technol.* **19**, 497 (2003).
34. Y. Birol: Effect of silicon content in grain refining hypoeutectic Al–Si founday alloys with boron and titanium additions. *Mater. Sci. Technol.* **28**, 385 (2012).
35. J.A. Spittle, J.M. Keeble, and M.A. Meshhedani: The grain refinement of Al–Si foundry alloy. *Light Met.*, 795 (1997).
36. X. Liu, Y. Liu, D. Huang, Q. Han, and X. Wang: Tailoring in situ TiB_2 particulates in aluminum matrix composites. *Mater. Sci. Eng., A* **705**, 55 (2017).
37. J. Røyse and N. Ryum: Scandium in aluminium alloys. *Int. Mater. Rev.* **50**, 19 (2005).
38. S.L. Pramod, A.K. Prasada Rao, B.S. Murty, and S.R. Bakshi: Effect of Sc addition on the microstructure and wear properties of A356 alloy and A356-TiB_2 in situ composite. *Mater. Des.* **78**, 85 (2015).
39. J. Fjellstedt, A. Jarfors, and L. Svendsen: Experimental analysis of the intermediary phase AlB_2, $AlB1_2$, and TiB_2 in the Al–B and Al–Ti–B systems. *J. Alloys Compd.* **283**, 192 (1999).
40. L. Arnberg, L. Backerud, and H. Klang: 1: Production and properties of master alloys of Al–Ti–B type and their ability to grain refine aluminum. *Cosmet. Technol.* **9**, 1 (1982).
41. T.E. Quested: Understanding mechanism of grain refinement of aluminium alloy by inoculation. *Mater. Sci. Technol.* **20**, 1357 (2004).
42. I. Maxwell and A. Hellawell: The constitution and aolidification of peritectic alloys in the system Al–Ti. *Acta Metall. Mater.* **23**, 895 (1975).
43. I. Maxwell and A. Hellawell: An analysis of the peritectic reaction with particular reference to Al–Ti alloys. *Acta Metall. Mater.* **23**, 901 (1975).
44. A.A. Abdel-Hamid, S. Hamar-Thibault, and R. Hamar: Crystal morphology of the compound TiB_2. *J. Cryst. Growth* **71**, 744 (1985).